Journal of Power Sources 188 (2009) 308–312

Contents lists available at ScienceDirect

Journal of Power Sources

journal homepage: www.elsevier.com/locate/jpowsour

Short communication

Nano-NiOOH prepared by splitting method as super high-speed charge/discharge cathode material for rechargeable alkaline batteries

Junqing Pan[a,*], Yanzhi Sun[a], Zihao Wang[a], Pingyu Wan[a], Yusheng Yang[a], Maohong Fan[b,**]

[a] State Key Laboratory of Chemical Resource Engineering, Beijing University of Chemical Technology, Beijing 100029, China
[b] School of Materials Science and Engineering, Georgia Institute of Technology, Atlanta, GA 30332, USA

ARTICLE INFO

Article history:
Received 27 August 2008
Received in revised form 30 October 2008
Accepted 20 November 2008
Available online 6 December 2008

Keywords:
NiOOH
Nanomaterials
Cathode
Rechargeable batteries

ABSTRACT

The present paper introduces a new method to prepare nano-NiOOH by oxidizing and cracking spherical $Ni(OH)_2$ of nano-structure in NaClO–NaOH solution. The prepared samples were characterized by X-ray powder diffraction (XRD), field emission scan electronic microscope (FESEM) and transmission electron microscopy (TEM). Results indicate that the synthesized sample is nano-NiOOH rod of 60–150 nm in width. The charge/discharge tests show that the nano-NiOOH cathode shows good cycling reversibility at high current density of 10,000 mA g^{-1}, provides a high capacity of 276 mAh g^{-1} and reduces the charge time to as short as 1.83 min. Furthermore, the nano-NiOOH still keeps a reversible capacity of 93.7% after 120 cycles at a super high charge/discharge current of 10,000 mA g^{-1}, showing a good charge/discharge property.

1. Introduction

With the fast development of portable electronic products over the past two decades, increasing importance has been attached to the high current charge/discharge characteristics of batteries. It is generally acknowledged that it is more difficult to engineer batteries capable of high-rate charging than high-rate discharging [1–9]. For example, existing technologies such as Ni-MH, Li-ion, and silver–zinc batteries can achieve high discharge rates up to 1–6 C, but the electric charge acceptance ability is so poor that longer than 1.4–10 h of charge time are needed.

The electrochemical transformation between $Ni(OH)_2$ and NiOOH, the most common redox couples of alkaline secondary batteries, is the basic principle of nickel-based batteries such as Ni-MH, Ni–Cd, and Edison batteries, which brings about an annual global production of over 3 billion pieces [10,11]. Compared with the large specific capacity of metal hydride (MH) anode, the limited charging capacity of $Ni(OH)_2$ cathode represents a barrier to the improvement of the properties of nickel batteries [12–15]. Up to now, conventional β-$Ni(OH)_2$ which can only provide a specific capacity of 150–170 mAh g^{-1} has been commonly used as a cathode material [16]. The synthesis and application of spherical nickel hydroxide dramatically increase the charge/discharge capacity of this cathode to above 230 mAh g^{-1} [17,18]. The discharge capacity of nano-$Ni(OH)_2$ electrodes prepared by ultrasonic chemistry, hard template method and other common methods can reach as high as 250 mAh g^{-1}, further approaching the theoretical capacity of 291 mAh g^{-1} calculated by Faraday's law [19–23]. However, mass production of nano-$Ni(OH)_2$ is impractical by using the hard template method.

In the primary battery field, the alkaline Zn/MnO_2 battery plays a dominant role due to its mature technology and competitive price, resulting in an annual worldwide production of 60 billion manganese batteries. However, the capacity of alkaline Zn/MnO_2 batteries declines severely under high current load [24]. By contrast, with substitution of high-performance spherical NiOOH for MnO_2, the Zn/NiOOH battery has achieved a high discharge current over 120 mA g^{-1}, offering a service life several times as long as that of alkaline Zn/MnO_2 batteries [25,26].

Considerable researches are conducted on the preparation and electrochemical performance of nano-nickel hydroxide in certain applications [27–29]. However, it is difficult to use the current methods to synthesize nanomaterials as NiOOH due to its strong oxidation property in strong alkaline solution. Consequently, little study has been carried out on the preparation and electrochemical properties of nano-NiOOH, and there is no attempt to report the nano-NiOOH rod with high performance at super high charge/discharge rates. Here we report a new

* Corresponding author. Tel.: +86 10 64449332; fax: +86 10 64449332.
** Corresponding author. Tel.: +307 766 5633; fax: +307 766 6777.
E-mail addresses: jqpan@mail.buct.edu.cn (J. Pan), mfan@mail.gatech.edu (M. Fan).

0378-7753/$ – see front matter.
doi:10.1016/j.jpowsour.2008.11.127

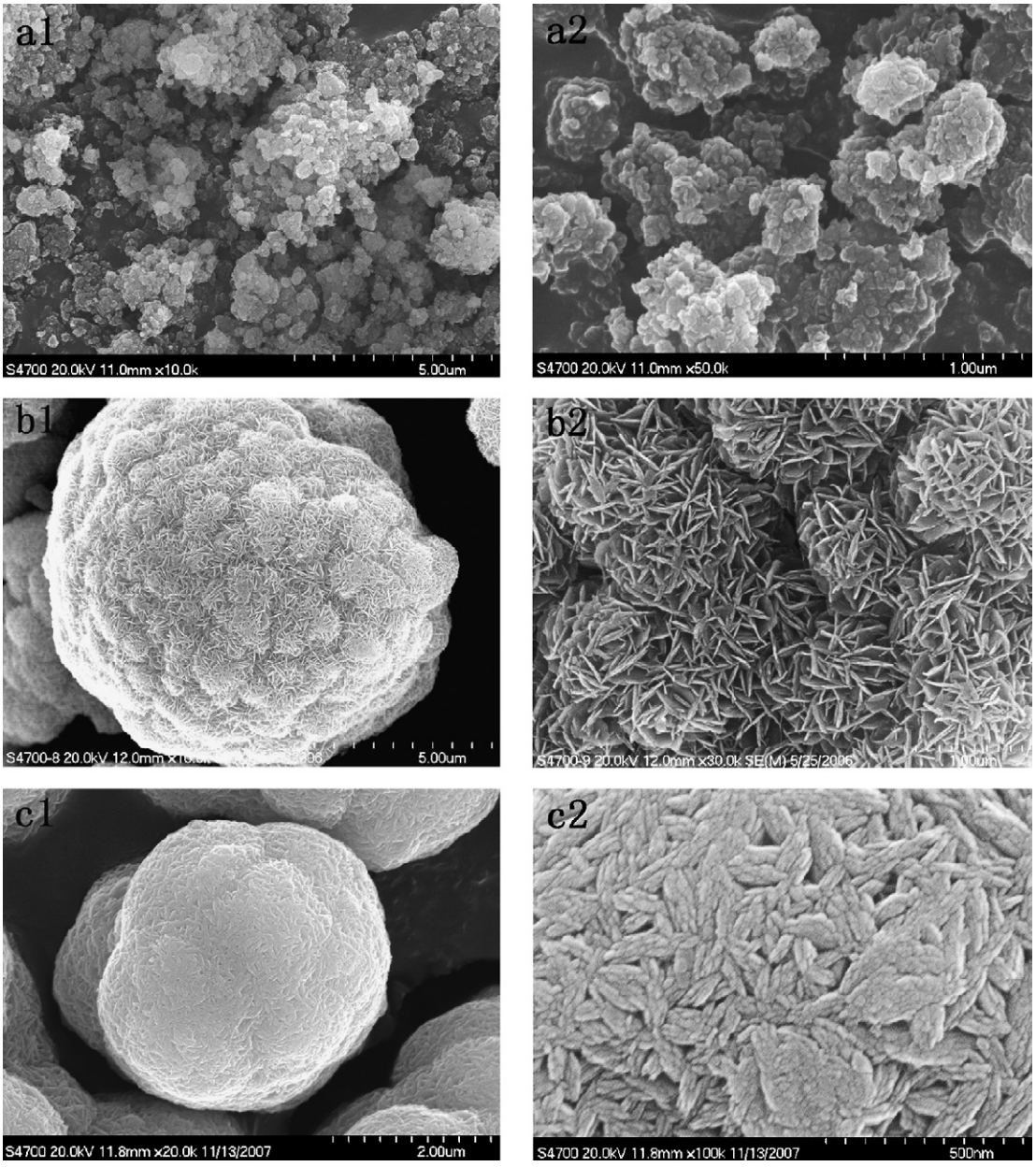

Fig. 1. The FSEM pictures of the $Ni(OH)_2$ samples at different pH (sample a: 10.90–11.05; sample b: 11.21–11.29; sample c: 11.40–11.60).

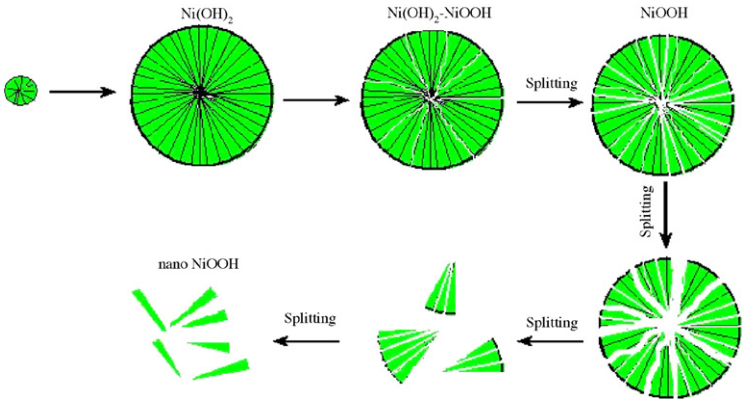

Fig. 2. The producing schematic diagram of the nano-NiOOH by splitting method.

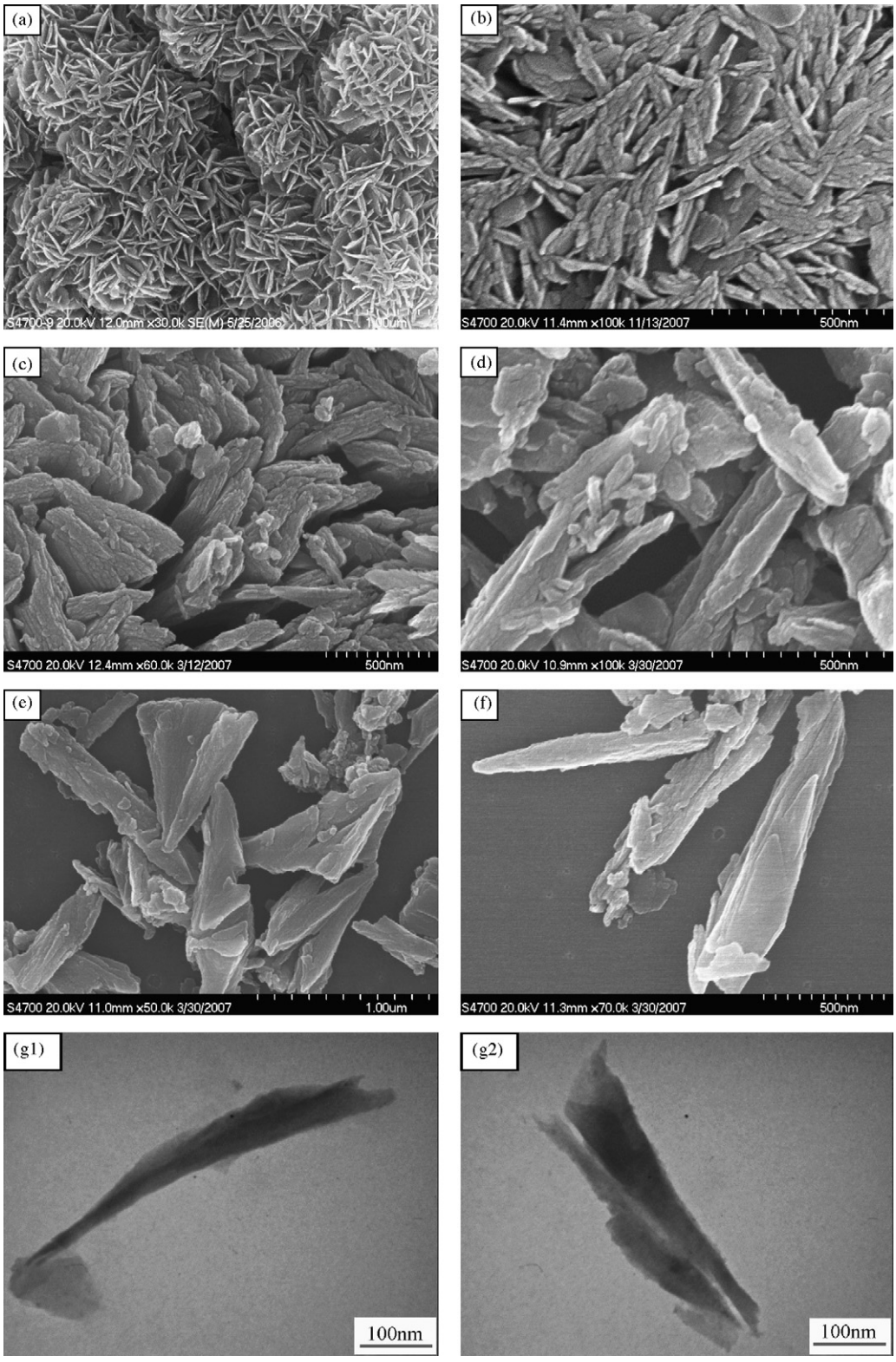

Fig. 3. The FSEM images of NiOOH samples prepared at different reaction time. (a) 0 h, (b) 2 h, (c) 4 h, (d) 6 h, (e) 9 h, (f) 12 h, and (g) is the TEM images of the NiOOH sample prepared for 12 h.

approach to the batch synthesis of nano-NiOOH rod by oxidizing and splitting nano-structured spherical nickel hydroxide. The prepared nano-NiOOH has good cycling reversibility at a super high current density of 10,000 mA g^{-1}, provides a high discharge capacity of 276.1 mAh g^{-1} and reduces the charge time to as short as 1.83 min.

2. Experimental

Mixed solution of 1.2 M $NiSO_4$, 0.01 M Na_2SO_4 and 0.02 M H_2SO_4 was prepared in a 100 ml volumetric flask, from which 50 ml was removed to a beaker in reserve and marked as solution A.

50 ml 3 M NaOH + 0.6 M NH_3 solution was marked as B.

8.5 ml 13.2 M ammonia was diluted to 100 ml and marked as solution C.

Solution C was removed into a reactor equipped with a heater, an agitator and a pH measurement device. Temperature was controlled at 52 °C. Solution A and B were slowly pumped into the reactor by using two constant flow pumps controlled by two microcomputers. Three samples, a, b and c, were separately obtained by controlling pH value within 10.90–11.05, 11.21–11.29 and 11.40–11.60, respectively. Flow volume was 0.40–0.41 ml min^{-1}. When the reaction was finished, stirring of the solution was maintained for 20 h, followed by removing out and washing the precipitation product with hot deionized water until the pH of filtered solution was within 7.1–7.6. Then the product was dried in vacuum at 60 °C for 3 h to obtain the samples.

A NaClO–NaOH solution was prepared using the method reported elsewhere [12]. 10 g of above prepared $Ni(OH)_2$ powders were then added to the NaClO–NaOH solution by stirring in the temperature range of 5–10 °C. A black NiOOH suspension formed after reacting for a period of 6–12 h was washed with deionized water using a decanting method and filtered using a G4 sintered glass filter. The precipitate was then dried in a 50 °C vacuum environment for 6 h, yielding the NiOOH samples. The purity of the NiOOH sample was analyzed by ferrous titration [12]. For the sake of contrast, the ordinary spheric $Ni(OH)_2$ as raw material was also added to the above concentrated sodium hypochlorite solution with constant agitation at 25–35 °C for 3 h to form spheric NiOOH [12].

The phase structure of the prepared NiOOH samples was analyzed using a Rigaku D/max2500VB2+/PCX X-ray diffractometer (XRD) with a Cu anticathode (40 kV, 200 mA). The morphology of the NiOOH samples was examined using a field emission scan electronic microscope (FESEM) and a transmission electron microscopy (TEM).

The nano-NiOOH electrodes were fabricated as described in detail elsewhere [3]. A pure nickel plate was used as an auxiliary cathode, a Zn(Hg)/ZnO electrode as reference electrode and 9 M KOH solution as the electrolyte. The charge/discharge performance of the prepared electrode was measured using a Land-2001A cell test instrument.

3. Results and discussions

Fig. 1 is FSEM photos of three types of $Ni(OH)_2$ (a, b, and c) obtained at different pH. It shows a great effect of pH on the morphology. It is hard to form spherical $Ni(OH)_2$ and there appears nano-grain even amorphous colloid at low pH (10.90–11.05), while dense spherical $Ni(OH)_2$ is easily formed at high pH (11.40–11.60). When pH is in an appropriate range(11.21–11.29), a balance between the complexation dissolution and precipitation is achieved, and the $Ni(OH)_2$ particles convert into abundant nano-$Ni(OH)_2$ flakes, piling up to form spherical nano-$Ni(OH)_2$ along a certain space direction. Thus, nano-NiOOH may be obtained by oxidizing and cracking nano-structured $Ni(OH)_2$.

Fig. 2 represents a schematic diagram for the production of nano-NiOOH using the splitting method mentioned above. Experiments in synthesizing NiOOH have revealed that proper concentrations of NaClO and NaOH, longer reaction time and higher reaction temperature can promote the decomposition of NaClO solution both on the surface and inside the spherical $Ni(OH)_2$. The tension of oxygen generated during the decomposition reaction will crack the spherical NiOOH to be split.

Fig. 3 shows FESEM and TEM images of the prepared NiOOH samples at different reaction time. It can be seen from Fig. 3a that the nano-structured spherical $Ni(OH)_2$ consists of numerous nanometer $Ni(OH)_2$ rods. In the process of reaction, cracks develop from the surface toward the core of spherical NiOOH until the sphere breaks into NiOOH rods. The results show that the NiOOH is completely split into rods after 12 h. Using the measuring scale in the diagram, it can be seen that the NiOOH rods range from 70 to 200 nm in width and 600 to 1000 nm in length. Fe^{2+} titration analysis indicates that the purity of nano-structured NiOOH is about 98.2%. TEM analysis (Fig. 3g_1 and g_2) reveals that the NiOOH sample prepared using the above-mentioned splitting method is typically in the shape of a rod or shuttle of 60–150 nm in width and 500–900 nm in length, conforming to the results of FESEM analysis.

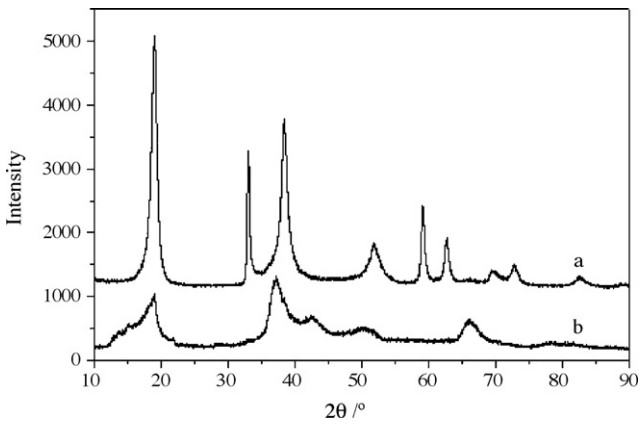

Fig. 4. The XRD patterns of the samples. (a) The spherical $Ni(OH)_2$ and (b) the prepared nano-NiOOH.

The XRD patterns of the prepared nano-NiOOH sample are shown in Fig. 4. By contrast to X-ray diffraction patterns mentioned elsewhere [12], the diffraction peak still proves the sample to be NiOOH. Moreover, the diffraction peak appears to widen significantly as a result of reducing the size of nano-NiOOH. The calculation shows 55.2 nm in particle diameter of the NiOOH rods. Therefore, NiOOH spheres can be split into large numbers of nano-structured rods by improving the reaction conditions.

Fig. 5 represents the first discharge curves of both spherical and nano-NiOOH with the same content of graphite (20 wt.%) as inert electronic conductor under different discharge current densities. It can be seen that the discharge capacity of nano-NiOOH (from 282.2 to 196.3 mAh g^{-1}) are much higher than that of spherical NiOOH (from 250.3 to 124.2 mAh g^{-1}) corresponding to an increase in discharge current density from 120 to 10,000 mA g^{-1}. Under conditions of 80X electric current density, the remaining ratio of discharge capacity in a nano-NiOOH electrode is about 69.3%.

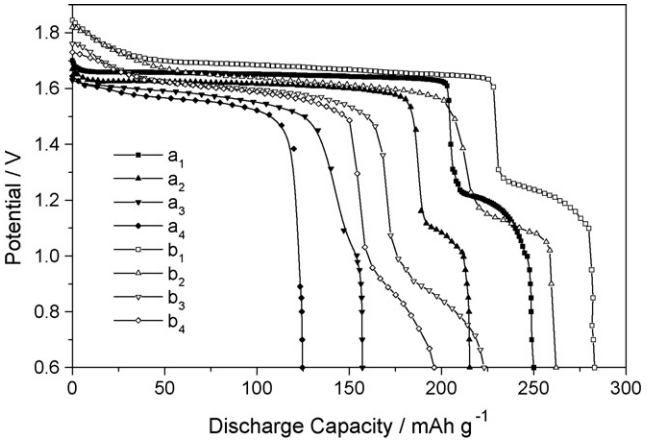

Fig. 5. Discharge curves of the NiOOH cathodes at different discharge current densities. (a) The spherical NiOOH and (b) the prepared nano-NiOOH. a_1 and b_1: 120 mA g^{-1}; a_2 and b_2: 1000 mA g^{-1}; a_3 and b_3: 5000 mA g^{-1}; a_4 and b_4: 10,000 mA g^{-1}.

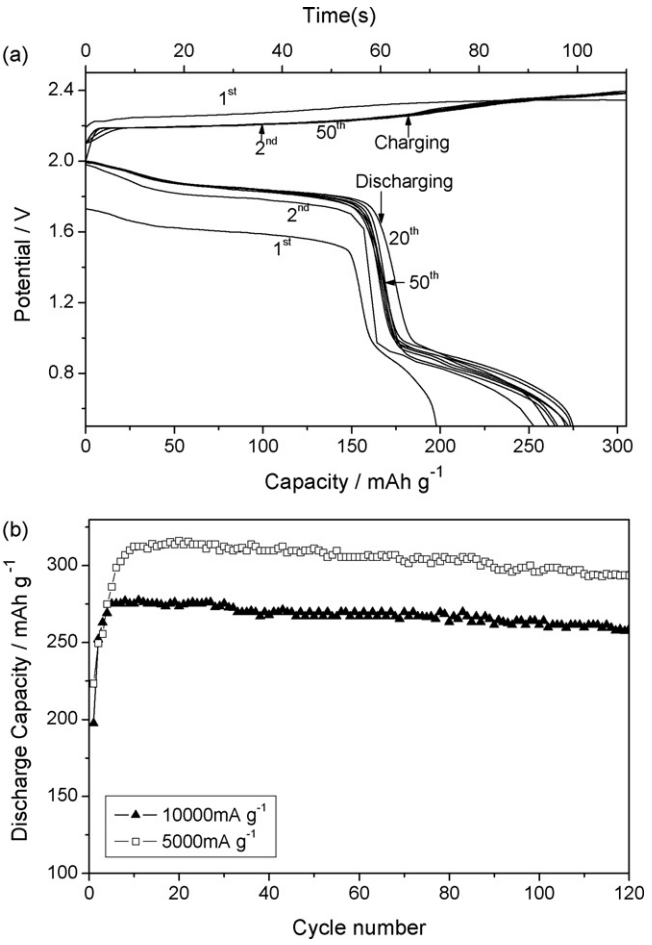

Fig. 6. (a) Discharge curve of nano-NiOOH under the super high charge/discharge rate of 10,000 mA g^{-1}. (b) Cycle stability of the nano-NiOOH cathodes at current density of 5000 and 10,000 mA g^{-1}.

By contrast, the discharge capacity of spherical NiOOH remains 124.2 mAh g^{-1}—only 49.6% of 250.3 mAh g^{-1} under a discharge current density of 120 mA g^{-1}. The super high current discharge properties of nano-NiOOH result from the fine size of its particles, accelerating the participation of most internal NiOOH in the reaction. Conversely, the greater size of spherical NiOOH prevents considerable quantities of internal NiOOH from quick entering the reaction, showing a longer and lower second plateau (1.1–1.2 V) during the discharge proceed. That decreases the high-rate discharge capacity.

Fig. 6a shows the charge/discharge curves of nano-NiOOH under a super high charge/discharge rate of 10,000 mA g^{-1}. It can be seen that the first 50 cycles of discharge curves are almost identical under a charge/discharge current density of 10,000 mA g^{-1}, thus suggesting that nano-NiOOH maintains relatively satisfactory cycling performance at super high charge/discharge rates. Experimental results indicate that nano-NiOOH achieves a cycling capacity of 276.1 mAh g^{-1}, reducing charge time of the electrode down to 1.83 min. This suggests that charging time for rechargeable alkaline batteries would be greatly reduced by the application of nano-NiOOH as a cathode material, making nickel rechargeable batteries much more efficient. Fig. 6b shows that a nano-NiOOH electrode can achieve discharge capacities of 315.2 and 276.1 mAh g^{-1} under charge/discharge current densities of 5000 and 10,000 mA g^{-1}, respectively, corresponding to respective retaining capacities of 94.0 and 93.7% after 120 cycles. No obvious decay in the cycling properties of nano-NiOOH electrodes is observed when they are charged and discharged at super-high rates, thus demonstrating that nano-NiOOH offers robust cycling characteristics.

4. Conclusion

In summary, a new method to prepare nano-NiOOH by oxidizing and cracking spherical $Ni(OH)_2$ in a NaClO–NaOH solution is reported in this article. The experimental results show that nano-NiOOH exhibits good cycling reversibility at super high current density of 10,000 mA g^{-1}, provides a high discharge capacity of 276.1 mAh g^{-1} and reduces the charge time to as short as 1.83 min. Furthermore, nano-NiOOH still maintains a reversible capacity of 93.7% after 120 cycles at a super high charge/discharge current of 10,000 mA g^{-1}, demonstrating good charge/discharge properties. We deduce that the excellent electrochemical performance of nano-NiOOH would make it possible as a promising candidate for the rapid refueling of electric automobiles, comparable to refueling rates for conventional internal combustion vehicles.

Acknowledgements

The authors gratefully acknowledge Prof. A. Manthiram (Materials Science and Engineering Program, University of Texas at Austin). This work was supported by “National Basic Research Program of China” (No. 2007CB210307), the Fund of CRE for New Faculty (NO. CRE-B-2008109) and National Natural Science Foundation of China (No. 20573135).

References

[1] Y.F. Yuan, J.P. Tu, H.M. Wu, Y. Li, D.Q. Shi, X.B. Zhao, J. Power Sources 159 (2006) 357.
[2] C.-Y. Seo, S.-J. Choi, J. Choi, C.-N. Park, P.S. Lee, J.-Y. Lee, Int. J. Hydrogen Energy 28 (2003) 317.
[3] J.Q. Pan, Y.Z. Sun, Z.H. Wang, P.Y. Wan, X.G. Liu, M.H. Fan, J. Mater. Chem. 17 (2007) 4820.
[4] H.B. Zhang, H.S. Liu, X.J. Cao, S.J. Li, C.C. Sun, Mater. Chem. Phys. 79 (2003) 37.
[5] J. Ren, Z. Zhou, X.P. Gao, J. Yan, Electrochim. Acta 52 (2006) 1120.
[6] X.W. Lou, Y. Wang, C.L. Yuan, J.Y. Lee, L.A. Archer, Adv. Mater. 18 (2006) 2325.
[7] F. Jiao, P.G. Bruce, Adv. Mater. 19 (2007) 657.
[8] K.R. Prasad, K. Koga, N. Miura, Chem. Mater. 16 (2004) 1845.
[9] S. Licht, B.H. Wang, S. Ghosh, Science 285 (1999) 1039.
[10] M. Stanley, M.S. Whittingham, Chem. Rev. 104 (2004) 4271.
[11] R.M. Dell, Solid State Ionics 134 (2000) 139.
[12] J.Q. Pan, Y.Z. Sun, P.Y. Wan, Z.H. Wang, X.G. Liu, Electrochem. Commun. 7 (2005) 857.
[13] Y.L. Zhao, J.M. Wang, H. Chen, T. Pan, J.Q. Zhang, C.N. Cao, Electrochim. Acta 50 (2004) 91.
[14] Q.S. Song, C.H. Chiu, S.L.I. Chan, Electrochim. Acta 51 (2006) 6548.
[15] H. Chen, J.M. Wang, T. Pan, Y.L. Zhao, J.Q. Zhang, C.N. Cao, J. Power Sources 143 (2005) 243.
[16] P. Oliva, J. Leonardi, J.F. Laurent, J. Power Sources 8 (1982) 229.
[17] J. Fan, Y.F. Yang, Y.B. Yang, H.X. Shao, Electrochim. Acta 53 (2007) 1979.
[18] Y.Z. Sun, J.Q. Pan, P.Y. Wan, C.C. Xu, X.G. Liu, Chin. J. Chem. Eng. 15 (2007) 262.
[19] J. Chen, N. Kuriyama, H. Yuan, H.T. Takeshita, T. Sakai, J. Am. Chem. Soc. 123 (2001) 11813.
[20] F.S. Cai, G.Y. Zhang, J. Chen, X.L. Gou, H.K. Liu, Angew. Chem. Int. Ed. 43 (2004) 4212.
[21] P. Jeevanandam, Y. Koltypin, A. Gedanken, Nano Lett. 1 (2001) 263.
[22] X.H. Liu, L. Yu, J. Power Sources 128 (2004) 326.
[23] X.M. He, J.J. Li, H.W. Cheng, C.Y. Jiang, C.R. Wan, J. Power Sources 152 (2005) 285.
[24] F.Y. Cheng, J. Chen, X.L. Gou, P.W. Shen, Adv. Mater. 17 (2005) 2753.
[25] X.Z. Fu, Q.C. Xu, R.Z. Hu, B.X. Pan, J.D. Lin, D.W. Liao, J. Power Sources 164 (2007) 916.
[26] X.Z. Fu, X. Wang, Q.C. Xu, J. Li, J.Q. Xu, J.D. Lin, D.W. Liao, Electrochim. Acta 52 (2007) 2109.
[27] L. Cao, F. Xu, Y.Y. Liang, H.L. Li, Adv. Mater. 16 (2004) 1853.
[28] X.J. Han, P. Xu, C.Q. Xu, L. Zhao, Z.B. Mo, T. Liu, Electrochim. Acta 50 (2005) 2763.
[29] Y. Lee, G.M. Morales, L.P. Yu, Angew. Chem. Int. Ed. 44 (2005) 2.